Smart Mater. Struct. 9 (2000) 389–401. Printed in the UK PII: S0964-1726(00)12007-5

Cement-matrix composites for smart structures

D D L Chung

Composite Materials Research Laboratory, State University of New York at Buffalo, Buffalo, NY 14260-4400, USA

Received 22 November 1999, in final form 21 January 2000

Abstract. Cement-matrix composites for smart structures are reviewed. The functions include strain sensing, damage sensing, temperature sensing, thermoelectricity, vibration reduction and radio wave reflection. The functions are rendered by the use of admixtures, such as short carbon fibers, short steel fibers and silica fume.

1. Introduction

Smart structures are important due to their relevance to hazard mitigation, structural vibration control, structural health monitoring, transportation engineering and thermal control. Research on smart structures has emphasized the incorporation of various devices in a structure for providing sensing, energy dissipation, actuation, control or other functions. Research on smart composites has emphasized the incorporation of a smart material in a matrix material for enhancing the smart function or the durability. Research on smart materials has emphasized the study of materials (e.g. piezoelectric materials) used for making the devices. However, relatively little attention has been given to the development of structural materials (e.g. concrete) that are inherently able to provide some of the smart functions, so that the need for embedded or attached devices is reduced or eliminated, thereby lowering cost, enhancing durability, increasing the functional volume and minimizing mechanical property degradation (which usually occurs in the case of embedded devices).

Smart structures are structures that have the ability to sense certain stimuli and be able to respond to the stimuli in an appropriate fashion. Sensing is the most fundamental aspect of a smart structure. A structural composite which is itself a sensor is multifunctional.

This article reviews cement-matrix structural composites for smart structures. The smart functions addressed include strain sensing (for structural vibration control and traffic monitoring), damage sensing (both mechanical and thermal damage in relation to structural health monitoring), temperature sensing (for thermal control, hazard mitigation and structural performance control), thermoelectricity (for thermal control and energy saving), vibration reduction (for structural vibration control) and electromagnetic radiation reflection (for lateral guidance in highways).

Cement-matrix composites include concrete (containing coarse and fine aggregates), mortar (containing fine aggregate, but no coarse aggregate) and cement paste (containing no aggregate, whether coarse or fine). Other fillers, called admixtures, can be added to the mix to improve the properties of the composite. Admixtures are discontinuous, so that they can be included in the mix. They can be particles, such as silica fume (a fine particulate) and latex (a polymer in the form of a dispersion). They can be short fibers, such as polymer, steel, glass or carbon fibers. They can be liquids such as methylcellulose aqueous solution, water-reducing agent, defoamer, etc. Admixtures for rendering the composite smart while maintaining or even improving the structural properties are the focus of this article.

2. Background on cement-matrix composites

Cement-matrix composites for smart structures include those containing short carbon fibers (for sensing strain, damage and temperature, for thermal control and for electromagnetic radiation reflection), short steel fibers (for sensing temperature and for thermal control) and silica fume (for vibration reduction). This section provides background on cement-matrix composites, with emphasis on carbon fiber cement-matrix composites due to its dominance among inherently smart cement-matrix composites.

Carbon-fiber cement-matrix composites are structural materials that are quite rapidly gaining in importance due to the decrease in carbon-fiber cost [1] and the increasing demand of superior structural and functional properties. These composites contain short carbon fibers, typically 5 mm in length, as the short fibers can be used as an admixture in concrete (whereas continuous fibers cannot be simply added to the concrete mix) and short fibers are less expensive than continuous fibers. However, due to the weak bond between the carbon fiber and the cement matrix, continuous fibers [2–4] are much more effective than short fibers in reinforcing concrete. Surface treatment of carbon fiber (e.g. by heating [5] or by using ozone [6, 7], silane [8], SiO_2 particles [9] or hot NaOH solution [10]) is useful for improving the bond between the fiber and the matrix, thereby improving the properties of the composite. In the case of surface treatment by ozone or silane, the improved bond is due to

0964-1726/00/040389+13$30.00

the enhanced wettability by water. Admixtures such as latex [6, 11] methylcellulose [6] and silica fume [12] also help the bond.

The effect of carbon-fiber addition on the properties of concrete increases with the fiber volume fraction [13], unless the fiber volume fraction is so high that the air void content becomes excessively high [14]. (The air void content increases with fiber content and air voids tend to have a negative effect on many properties, such as the compressive strength.) In addition, the workability of the mix decreases with fiber content [13]. Moreover, the cost increases with fiber content. Therefore, a rather low volume fraction of fibers is desirable. A fiber content as low as 0.2 vol% is effective [15], although fiber contents exceeding 1 vol% are more common [16–20]. The required fiber content increases with the particle size of the aggregate, as the flexural strength decreases with increasing particle size [21].

Effective use of the carbon fibers in concrete requires dispersion of the fibers in the mix. The dispersion is enhanced by using silica fume (a fine particulate) as an admixture [14, 22–24]. A typical silica fume content is 15% by weight of cement [14]. The silica fume is typically used along with a small amount (0.4% by weight of cement) of methylcellulose for helping the dispersion of the fibers and the workability of the mix [14]. Latex (typically 15–20% by weight of cement) is much less effective than silica fume for helping the fiber dispersion, but it enhances the workability, flexural strength, flexural toughness, impact resistance, frost resistance and acid resistance [14, 25, 26]. The ease of dispersion increases with decreasing fiber length [24].

The improved structural properties rendered by carbon-fiber addition pertain to the increased tensile and flexible strengths, the increased tensile ductility and flexural toughness, the enhanced impact resistance, the reduced drying shrinkage and the improved freeze–thaw durability [13–15, 17–25, 27–38]. The tensile and flexural strengths decrease with increasing specimen size, such that the size effect becomes larger as the fiber length increases [39]. The low drying shrinkage is valuable for large structures and for use in repair [40, 41] and in joining bricks in a brick structure [42, 43]. The functional properties rendered by carbon-fiber addition pertain to the strain sensing ability [7, 44–58] (for smart structures), the temperature sensing ability [59–62], the damage sensing ability [44, 48, 63–65], the thermoelectric behavior [60–62], the thermal insulation ability [66–68] (to save energy for buildings), the electrical conduction ability [69–78] (to facilitate cathodic protection of embedded steel and to provide electrical grounding or connection), and the radio wave reflection/absorption ability [79–83] (for electromagnetic interference or EMI shielding, for lateral guidance in automatic highways, and for television image transmission).

In relation to the structural properties, carbon fibers compete with glass, polymer and steel fibers [18, 27–29, 32, 36–38, 84]. Carbon fibers (isotropic pitch based) [1, 84] are advantageous in their superior ability to increase the tensile strength of concrete, even though the tensile strength, modulus and ductility of the isotropic pitch based carbon fibers are low compared to most other fibers. Carbon fibers are also advantageous in the relative chemical inertness [85]. Polyacrylonitrile(PAN)-based carbon fibers are also used [17, 19, 22, 33], although they are more commonly used as continuous fibers than short fibers. Carbon-coated glass fibers [86, 87] and submicrometer diameter carbon filaments [77–79] are even less commonly used, although the former is attractive for the low cost of glass fibers and the latter is attractive for its high radio wave reflectivity (which results from the skin effect). C-shaped carbon fibers are more effective for strengthening than round carbon fibers [88], but their relatively large diameter makes them less attractive. Carbon fibers can be used in concrete together with steel fibers, as the addition of short carbon fibers to steel-fiber-reinforced mortar increases the fracture toughness of the interfacial zone between the steel fiber and the cement matrix [89]. Carbon fibers can also be used in concrete together with steel bars [90, 91], or together with carbon-fiber-reinforced polymer rods [92].

In relation to most functional properties, carbon fibers are exceptional compared to the other fiber types. Carbon fibers are electrically conducting, in contrast to glass and polymer fibers, which are not conducting. Steel fibers are conducting, but their typical diameter ($\geqslant$60 μm) is much larger than the diameter of a typical carbon fiber (15 μm). The combination of electrical conductivity and small diameter makes carbon fibers superior to the other fiber types in the area of strain sensing and electrical conduction. However, carbon fibers are inferior to steel fibers for providing thermoelectric composites, due to the high electron concentration in steel and the low hole concentration in carbon.

Although carbon fibers are thermally conducting, addition of carbon fibers to concrete lowers the thermal conductivity [66], thus allowing applications related to thermal insulation. This effect of carbon-fiber addition is due to the increase in air void content. The electrical conductivity of carbon fibers is higher than that of the cement matrix by about eight orders of magnitude, whereas the thermal conductivity of carbon fibers is higher than that of the cement matrix by only one or two orders of magnitude. As a result, the electrical conductivity is increased upon carbon-fiber addition in spite of the increase in air void content, but the thermal conductivity is decreased upon fiber addition.

The use of pressure after casting [93], and extrusion [94, 95] can result in composites with superior microstructure and properties. Moreover, extrusion improves the shapability [95].

3. Cement-matrix composites for strain sensing

The electrical resistance of strain-sensing concrete (without embedded or attached sensors) changes reversibly with strain, such that the gage factor (fractional change in resistance per unit strain) is up to 700 under compression or tension [7, 44–58]. The resistance (dc/ac) increases reversibly upon tension and decreases reversibly upon compression, due to fiber pull-out upon microcrack opening ($<$1 μm) and the consequent increase in fiber matrix contact resistivity. This concrete contains as low as 0.2 vol% short carbon fibers, which are preferably those that have been surface treated. The fibers do not need to touch one another in the composite. The treatment improves the wettability with water. The presence

of a large aggregate decreases the gage factor, but the strain sensing ability remains sufficient for practical use. Strain-sensing concrete works even when data acquisition is wireless. The applications include structural vibration control and traffic monitoring.

Figure 1(*a*) shows the fractional change in resistivity along the stress axis as well as the strain during repeated compressive loading at an increasing stress amplitude for a carbon-fiber latex cement paste at 28 days of curing. Figure 1(*b*) shows the corresponding variation of stress and strain during the repeated loading. The strain varies linearly with the stress up to the highest stress amplitude (figure 1(*b*)). The strain returns to zero at the end of each cycle of loading. The resistivity decreases upon loading in every cycle (due to fiber push-in) and increases upon unloading in every cycle (due to fiber pull-out). The resistivity has a net increase after the first cycle, due to damage. Little further damage occurs in subsequent cycles, as shown by the resistivity after unloading not increasing much after the first cycle. The greater the strain amplitude, the more is the resistivity decrease during loading, although the resistivity and strain are not linearly related. The effects of figure 1 were similarly observed in a carbon-fiber silica-fume cement paste at 28 days of curing.

Figures 2 and 3 show the fractional changes in the longitudinal and transverse resistivities respectively for a carbon-fiber silica-fume cement paste at 28 days of curing during repeated unaxial tensile loading at increasing strain amplitudes. The strain essentially returns to zero at the end of each cycle, indicating elastic deformation. The longitudinal strain is positive (i.e. elongation); the transverse strain is negative (i.e. shrinkage due to the Poisson effect). Both longitudinal and transverse resistivities increase reversibly upon uniaxial tension. The reversibility of both strain and resistivity is more complete in the longitudinal direction than the transverse direction. The gage factor is 89 and −59 for the longitudinal and transverse resistances, respectively.

Figures 4 and 5 show corresponding results for a silica-fume cement paste. The strain is, essentially, totally reversible in both the longitudinal and transverse directions, but the resistivity is only partly reversible in both directions, in contrast to the reversibility of the resistivity when fibers are present (figures 2 and 3). As in the case with fibers, both longitudinal and transverse resistivities increase upon uniaxial tension. However, the gage factor is only 7.2 and −7.1 for figures 4 and 5, respectively.

Comparison of figures 2 and 3 (with fibers) with figures 4 and 5 (without fibers) shows that fibers greatly enhance the magnitude and reversibility of the resistivity effect. The gage factors are much smaller in magnitude when fibers are absent.

The increase in both the longitudinal and transverse resistivities upon uniaxial tension for cement pastes, whether with or without fibers, is attributed to defect (e.g. microcrack) generation. In the presence of fibers, fiber bridging across microcracks occurs and slight fiber pull-out occurs upon tension, thus enhancing the possibility of microcrack closing and causing more reversibility in the resistivity change. The fibers are much more electrically conductive than the cement matrix. The presence of the fibers introduces interfaces between the fibers and the matrix. The degradation of the fiber–matrix interface due to fiber pull-out or other mechanisms is an additional type of defect generation that will increase the resistivity of the composite. Therefore, the presence of fibers greatly increases the gage factor.

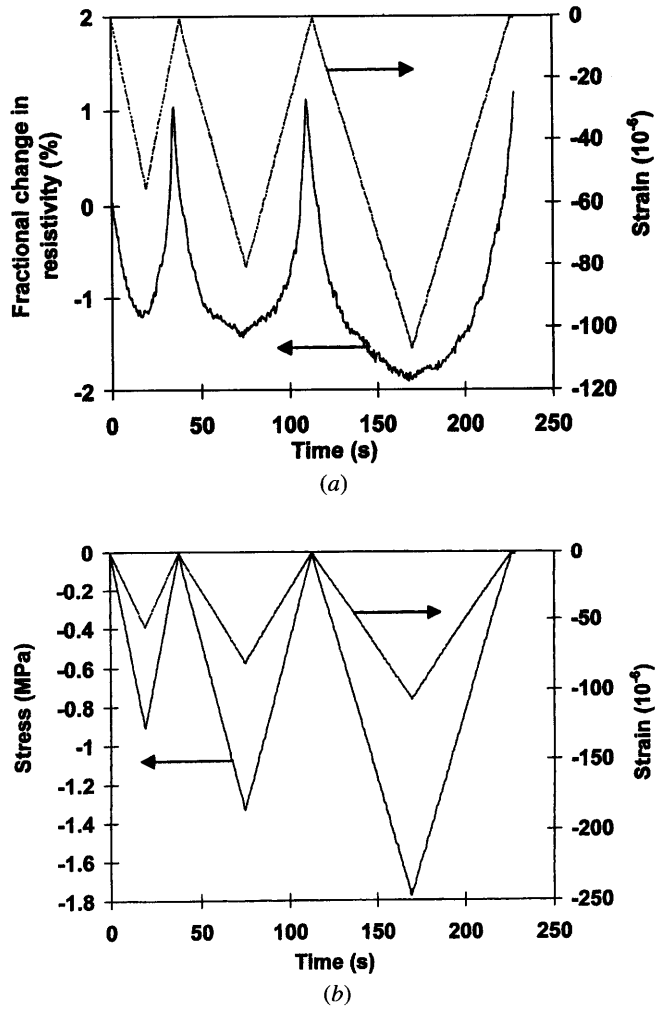

Figure 1. Variation of the fractional change in volume electrical resistivity with time (*a*), of the stress with time (*b*) and of the strain (negative for compressive strain) with time (*a*) and (*b*) during dynamic compressive loading at increasing stress amplitudes within the elastic regime for a carbon-fiber latex cement paste at 28 days of curing.

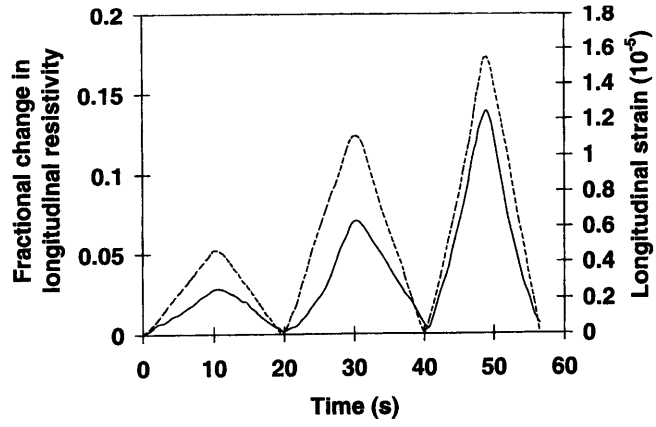

Figure 2. Variation of the fractional change in longitudinal electrical resistivity with time (full curve) and of the strain with time (broken curve) during dynamic uniaxial tensile loading at increasing stress amplitudes within the elastic regime for a carbon-fiber silica-fume cement paste.

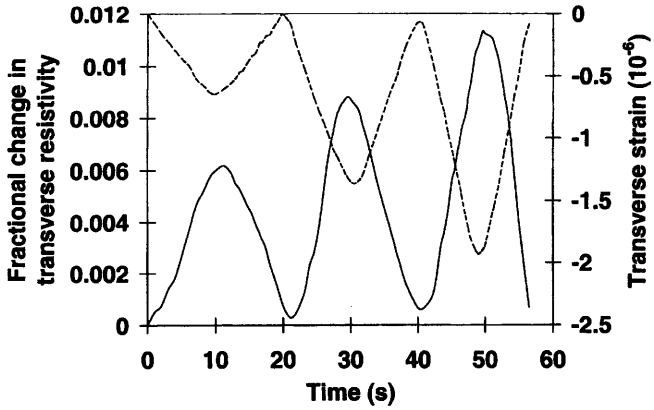

Figure 3. Variation of the fractional change in transverse electrical resistivity with time (full curve) and of the strain with time (broken curve) during dynamic uniaxial tensile loading at increasing stress amplitudes within the elastic regime for a carbon-fiber silica-fume cement paste.

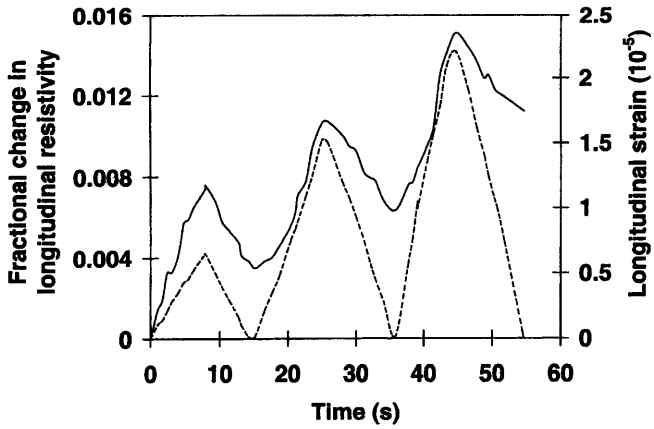

Figure 4. Variation of the fractional change in longitudinal electrical resistivity with time (full curve) and of the strain with time (broken curve) during dynamic uniaxial tensile loading at increasing stress amplitudes within the elastic regime for a silica-fume cement paste.

The transverse resistivity increases upon uniaxial tension, even though the Poisson effect causes the transverse strain to be negative. This means that the effect of the transverse resistivity increase overshadows the effect of the transverse shrinkage. The resistivity increase is a consequence of the uniaxial tension. In contrast, under uniaxial compression, the resistance in the stress direction decreases at 28 days of curing. Hence, the effects of uniaxial tension on the transverse resistivity and of uniaxial compression on the longitudinal resistivity are different; the gage factors are negative and positive for these cases, respectively.

The similarity of the resistivity change in the longitudinal and transverse directions under uniaxial tension suggests similarity for other directions as well. This means that the resistance can be measured in any direction in order to sense the occurrence of tensile loading. Although the gage factor is comparable in both longitudinal and transverse directions, the fractional change in resistance under uniaxial tension is much higher in the longitudinal direction than the transverse direction. Thus, the use of the longitudinal resistance for practical self-sensing is preferred.

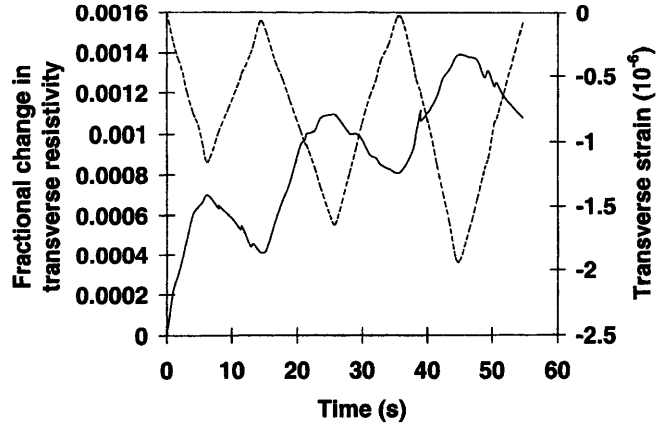

Figure 5. Variation of the fractional change in transverse electrical resistivity with time (full curve) and of the strain with time (broken curve) during dynamic uniaxial tensile loading at increasing stress amplitudes within the elastic regime for a silica-fume cement paste.

4. Cement-matrix composites for damage sensing

Concrete, whether with or without admixtures, is capable of sensing major and minor damage—even damage during elastic deformation—due to the electrical resistivity increase that accompanies damage [44, 48, 63–65]. That both strain and damage can be sensed simultaneously through resistance measurement means that the strain/stress condition (during dynamic loading) under which damage occurs can be obtained, thus facilitating damage origin identification. Damage is indicated by a resistance increase, which is larger and less reversible when the stress amplitude is higher. The resistance increase can be a sudden increase during loading. It can also be a gradual shift of the baseline resistance.

Figure 6(*a*) [64] shows the fractional change in resistivity along the stress axis as well as the strain during repeated compressive loading at an increasing stress amplitude for plain cement paste at 28 days of curing. Figure 6(*b*) shows the corresponding variation of stress and strain during the repeated loading. The strain varies linearly with the stress up to the highest stress amplitude (figure 6(b)). The strain returns to zero at the end of each cycle of loading. During the first loading, the resistivity increases due to damage initiation. During the subsequent unloading, the resistivity continues to increase, probably due to the opening of the microcracks generated during loading. During the second loading, the resistivity decreases slightly as the stress increases up to the maximum stress of the first cycle (probably due to closing of the microcracks) and then increases as the stress increases beyond this value (probably due to the generation of additional microcracks). During unloading in the second cycle, the resistivity increases significantly (probably due to the opening of the microcracks).During the third loading, the resistivity essentially does not change (or decreases very slightly) as the stress increases to the maximum stress of the third cycle (probably due to the balance between microcrack generation and microcrack closing). Subsequent unloading causes the resistivity to increase very significantly (probably due to the opening of the microcracks).

Figure 7 shows the fractional change in resistance, strain and stress during repeated compressive loading at

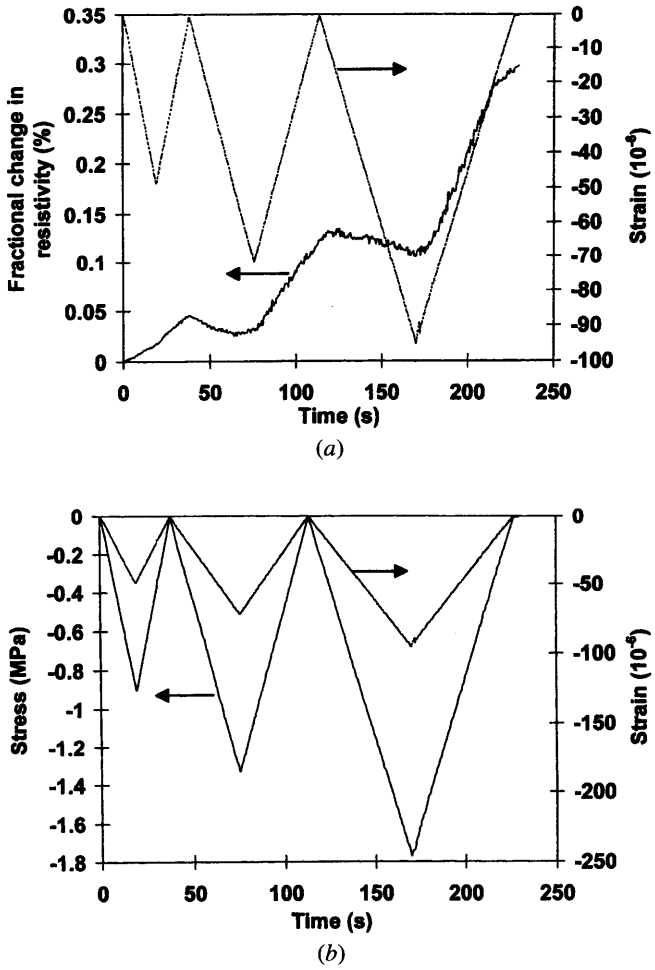

Figure 6. Variation of the fractional change in electrical resistivity with time (*a*), of the stress with time (*b*), and of the strain (negative for compressive strain) with time (*a*) and (*b*) during dynamic compressive loading at increasing stress amplitudes within the elastic regime for a silica-fume cement paste at 28 days of curing.

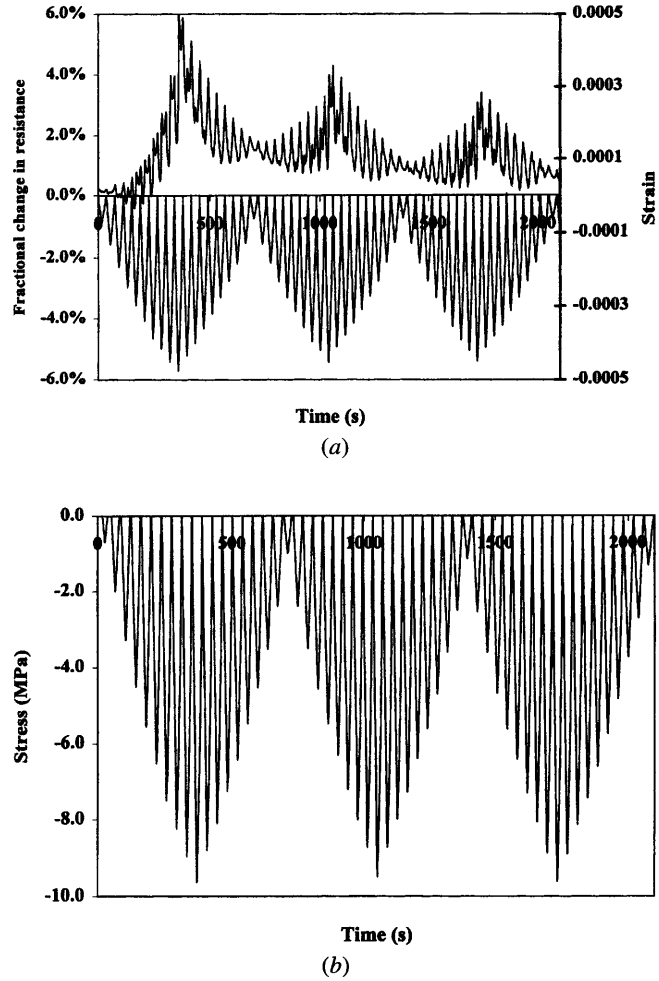

Figure 7. Fractional change in resistance (*a*), strain (*a*) and stress (*b*) during repeated compressive loading at increasing and decreasing stress amplitudes, the highest of which was 60% of the compressive strength, for carbon fiber concrete at 28 days of curing.

increasing and decreasing stress amplitudes for carbon-fiber (0.18 vol%) concrete (with fine and coarse aggregates) at 28 days of curing. The highest stress amplitude is 60% of the compressive strength. A group of cycles in which the stress amplitude increases cycle by cycle and then decreases cycle by cycle back to the initial low-stress amplitude is hereby referred to as a group. Figure 7 shows the results for three groups. The strain returns to zero at the end of each cycle for any of the stress amplitudes, indicating elastic behavior. The resistance decreases upon loading in each cycle, as in figure 1. An extra peak at the maximum stress of a cycle grows as the stress amplitude increases, resulting in two peaks per cycle. The original peak (strain induced) occurs at zero stress, while the extra peak (damage induced) occurs at the maximum stress. Hence, during loading from zero stress within a cycle, the resistance drops and then increases sharply, reaching the maximum resistance of the extra peak at the maximum stress of the cycle. Upon subsequent unloading, the resistance decreases and then increases as unloading continues, reaching the maximum resistance of the original peak at zero stress. In the part of this group where the stress amplitude decreases cycle by cycle, the extra peak diminishes and disappears, leaving the original peak as the sole peak. In the part of the second group, where the stress amplitude increases cycle by cycle, the original peak (peak at zero stress) is the sole peak, except that the extra peak (peak at the maximum stress) returns in a minor way (more minor than in the first group) as the stress amplitude increases. The extra peak grows as the stress amplitude increases, but, in the part of the second group in which the stress amplitude decreases cycle by cycle, it quickly diminishes and vanishes, as in the first group. Within each group, the amplitude of resistance variation increases as the stress amplitude increases and decreases as the stress amplitude subsequently decreases.

The greater the stress amplitude, the larger and the less reversible is the damage-induced resistance increase (the extra peak). If the stress amplitude has been experienced before, the damage-induced resistance increase (the extra peak) is small, as shown by comparing the result of the second group with that of the first group (figure 7), unless the extent of damage is large (figure 8 for a highest stress amplitude of >90% of the compressive strength). When the damage is extensive (as shown by a modulus decrease), damage-induced resistance increase occurs in every cycle, even at a decreasing stress amplitude, and it can overshadow the strain-induced resistance decrease (figure 8). Hence, the damage-induced resistance increase occurs mainly during loading (even within

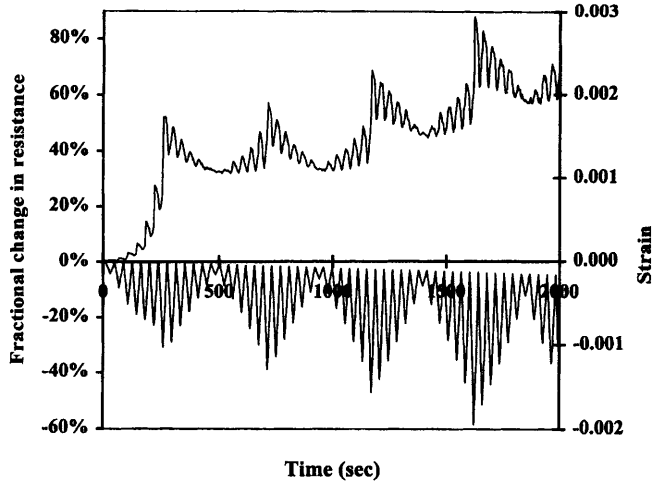

(*a*)

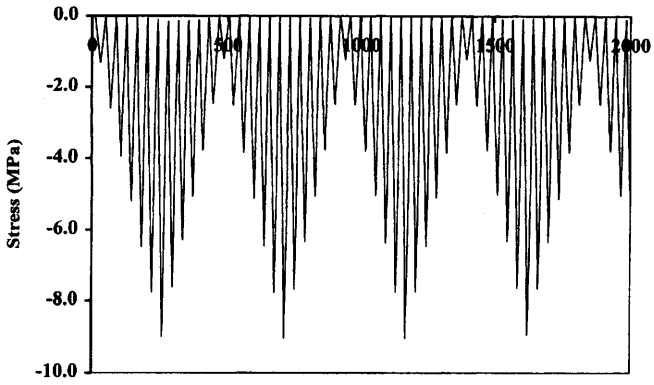

(*b*)

Figure 8. Fractional change in resistance (*a*), strain (*a*) and stress (*b*) during repeated compressive loading at increasing and decreasing stress amplitudes, the highest of which was >90% of the compressive strength, for a carbon-fiber concrete at 28 days of curing.

the elastic regime), particularly at a stress above that in prior cycles, unless the stress amplitude is high and/or damage is extensive.

At a high stress amplitude, the damage-induced resistance increase, cycle by cycle as the stress amplitude increases, causes the baseline resistance to increase irreversibly (figure 8). The baseline resistance in the regime of major damage (with a decrease in modulus) provides a measure of the extent of damage (i.e. condition monitoring). This measure works in the loaded or unloaded state. In contrast, the measure using the damage-induced resistance increase (figure 7) works only during stress increase and indicates the occurrence of damage (whether minor or major) as well as the extent of damage.

5. Cement-matrix composites for temperature sensing

A thermistor is a thermometric device consisting of a material (typically a semiconductor, but in this case a cement paste) whose electrical resistivity decreases with a rise in temperature. The carbon-fiber concrete described

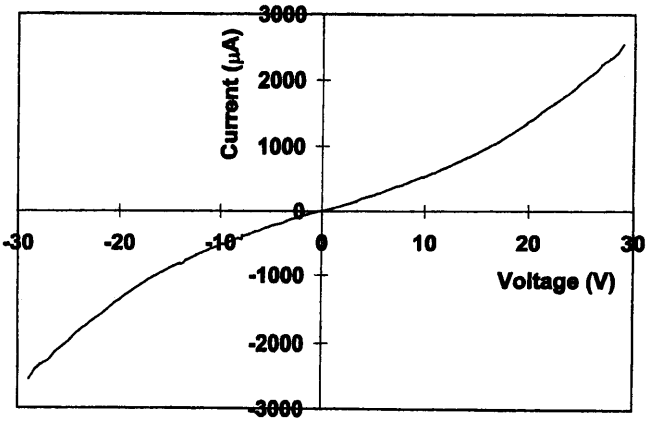

Figure 9. Current–voltage characteristic of a carbon-fiber silica-fume cement paste at 38 °C during stepped heating.

in section 3 for strain sensing is a thermistor due to its resistivity decreasing reversibly with increasing temperature [59]; the sensitivity is comparable to that of semiconductor thermistors. (The effect of temperature will need to be compensated in using the concrete as a strain sensor; section 3.)

Figure 9 [59] shows the current–voltage characteristic of a carbon-fiber (0.5% by weight of cement) silica-fume (15% by weight of cement) cement paste at 38 °C during stepped heating. The characteristic is linear below 5 V and deviates positively from linearity beyond 5 V. The resistivity is obtained from the slope of the linear portion. The voltage at which the characteristic starts to deviate from linearity is referred to as the critical voltage.

Figure 10 shows a plot of the resistivity against temperature during heating and cooling for a carbon-fiber silica-fume cement paste. The resistivity decreases upon heating and the effect is quite reversible upon cooling. That the resistivity is slightly increased after a heating–cooling cycle is probably due to thermal degradation of the material. Figure 11 shows the Arrhenius plot of log conductivity (conductivity = 1/resistivity) against the reciprocal absolute temperature. The slope of the plot gives the activation energy, which is 0.390 ± 0.014 and 0.412 ± 0.017 eV during heating and cooling, respectively.

Results similar to those of a carbon-fiber silica-fume cement paste were obtained with a carbon-fiber (0.5% by weight of cement) latex (20% by weight of cement) cement paste, a silica-fume cement paste, a latex cement paste and a plain cement paste. However, for all these four types of cement paste, (i) the resistivity is higher by about an order of magnitude and (ii) the activation energy is lower by about an order of magnitude, as shown in table 1. The critical voltage is higher when fibers are absent (table 1).

The Seebeck [60–62, 96] effect is a thermoelectric effect which is the basis for thermocouples for temperature measurement. This effect involves charge carriers moving from a hot point to a cold point within a material, thereby resulting in a voltage difference between the two points. The Seebeck coefficient is the voltage difference per unit temperature difference between the two points. Negative carriers (electrons) make it more positive and positive carriers (holes) make it more negative.

Table 1. Resistivity, critical voltage and activation energy of five types of cement paste.

Formulation	Resistivity at 20 °C (Ω cm)	Critical voltage at 20 °C (V)	Activation energy (eV)	
			Heating	Cooling
Plain	$(4.87 \pm 0.37) \times 10^5$	10.80 ± 0.45	0.040 ± 0.006	0.122 ± 0.006
Silica fume	$(6.12 \pm 0.15) \times 10^5$	11.60 ± 0.37	0.035 ± 0.003	0.084 ± 0.004
Carbon fibers and silica fume	$(1.73 \pm 0.08) \times 10^4$	8.15 ± 0.34	0.390 ± 0.014	0.412 ± 0.017
Latex	$(6.99 \pm 0.12) \times 10^5$	11.80 ± 0.31	0.017 ± 0.001	0.025 ± 0.002
Carbon fibers and latex	$(9.64 \pm 0.08) \times 10^4$	8.76 ± 0.35	0.018 ± 0.001	0.027 ± 0.002

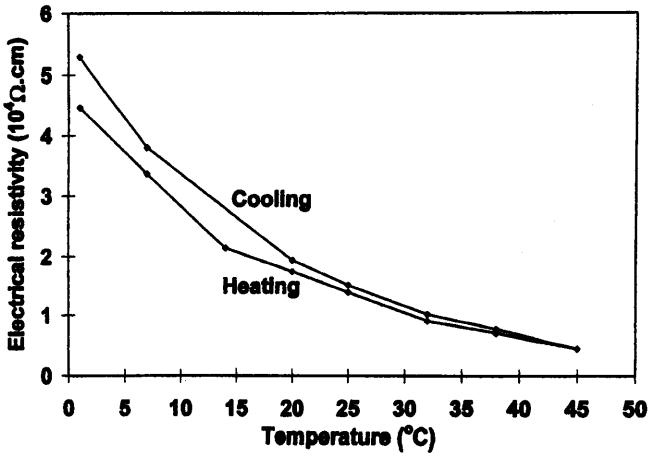

Figure 10. Plot of volume electrical resistivity against temperature during heating and cooling for a carbon-fiber silica-fume cement paste.

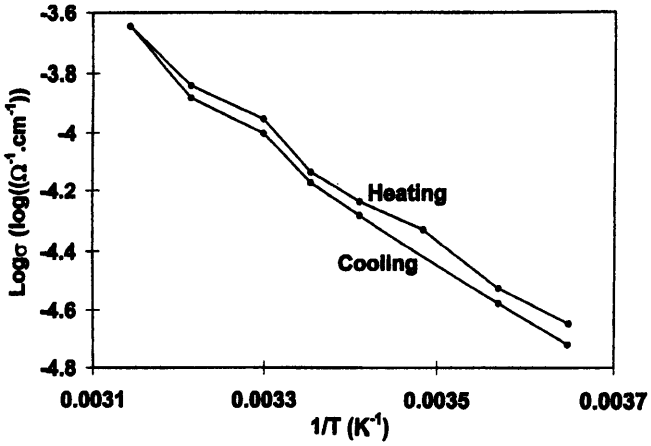

Figure 11. Arrhenius plot of log electrical conductivity against reciprocal absolute temperature for a carbon-fiber silica-fume cement paste.

The Seebeck effect in carbon-fiber-reinforced cement paste involves electrons from the cement matrix [62] and holes from the fibers [60, 61], such that the two contributions are equal at the percolation threshold; with a fiber content between 0.5% and 1.0% by weight of cement [62]. The hole contribution increases monotonically with increasing fiber content below and above the percolation threshold [62].

Due to the free electrons in a metal, a cement containing metal fibers such as steel fibers is even more positive in the thermoelectric power than a cement without fiber [96]. The attainment of a very positive thermoelectric power is attractive, since a material with a positive thermoelectric

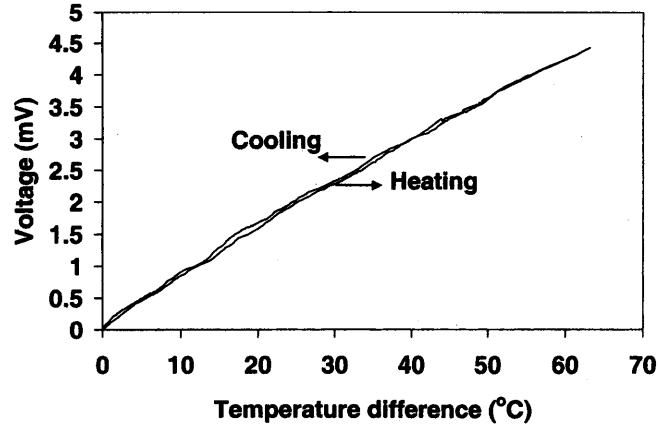

Figure 12. Variation of the Seebeck voltage (with copper as the reference) against the temperature difference during heating and cooling for a steel-fiber silica-fume cement paste containing steel fibers in the amount of 1.0% by weight of cement.

power and a material with negative thermoelectric power are two very dissimilar materials, the junction of which is a thermocouple junction. (The greater the dissimilarity, the more sensitive is the thermocouple.)

Table 2 and figure 12 show the thermopower results. The absolute thermoelectric power is much more positive for all the steel-fiber cement pastes compared to all of the carbon-fiber cement pastes. An increase of the steel-fiber content from 0.5% to 1.0% by weight of cement increases the absolute thermoelectric power, whether silica fume (or latex) is present or not. An increase of the steel-fiber content also increases the reversibility and linearity of the change in Seebeck voltage with the temperature difference between the hot and cold ends, as shown by comparing the values of the Seebeck coefficient obtained during heating and cooling in table 2. The values obtained during heating and cooling are close for the pastes with the higher steel-fiber content, but are not so close for the pastes with the lower steel-fiber content. In contrast, for pastes with carbon fibers in place of steel fibers, the change in the Seebeck voltage with the temperature difference is highly reversible for both carbon-fiber contents of 0.5% and 1.0% by weight of cement, as shown in table 2 by comparing the values of the Seebeck coefficient obtained during heating and cooling.

Table 2 shows that the volume electrical resistivity is much higher for the steel-fiber cement pastes than the corresponding carbon-fiber cement pastes. This is attributed to the much lower volume fraction of fibers in the former (table 2). An increase in the steel- or carbon-fiber content from 0.5% to 1.0% by weight of cement decreases the resistivity, although the decrease is more significant for the

Table 2. Volume electical resistivity, Seebeck coefficient ($\mu V\,°C^{-1}$), with copper as the reference, and the absolute thermoelectric power ($\mu V\,°C^{-1}$) of various cement pastes with steel fibers (S_f) or carbon fibers (C_f).

			Heating		Cooling	
Cement paste % by weight of cement	Volume fraction fibers	Resistivity (Ω cm)	Seebeck coefficient	Absolute thermoelectric power	Seebeck coefficient	Absolute thermoelectric power
$S_f(0.5)$	0.10%	$(7.8 \pm 0.5) \times 10^4$	51.0 ± 4.8	53.3 ± 4.8	45.3 ± 4.4	47.6 ± 4.4
$S_f(1.0)$	0.20%	$(4.8 \pm 0.4) \times 10^4$	56.8 ± 5.2	59.1 ± 5.2	53.7 ± 4.9	56.0 ± 4.9
$S_f(0.5)$ + silica fume	0.10%	$(5.6 \pm 0.5) \times 10^4$	54.8 ± 3.9	57.1 ± 3.9	52.9 ± 4.1	55.2 ± 4.1
$S_f(1.0)$ + silica fume	0.20%	$(3.2 \pm 0.3) \times 10^4$	66.2 ± 4.5	68.5 ± 4.5	65.6 ± 4.4	67.9 ± 4.4
$S_f(0.5)$ + latex	0.085%	$(1.4 \pm 0.1) \times 10^5$	48.1 ± 3.2	50.4 ± 3.2	45.4 ± 2.9	47.7 ± 2.9
$S_f(1.0)$ + latex	0.17%	$(1.1 \pm 0.1) \times 10^5$	55.4 ± 5.0	57.7 ± 5.0	54.2 ± 4.5	56.5 ± 4.5
$C_f(0.5)$ + silica fume	0.48%	$(1.5 \pm 0.1) \times 10^4$	-1.45 ± 0.09	0.89 ± 0.09	-1.45 ± 0.09	0.89 ± 0.09
$C_f(1.0)$ + silica fume	0.95%	$(8.3 \pm 0.5) \times 10^2$	-2.82 ± 0.11	-0.48 ± 0.11	-2.82 ± 0.11	-0.48 ± 0.11
$C_f(0.5)$ + latex	0.41%	$(9.7 \pm 0.6) \times 10^4$	-1.20 ± 0.05	1.14 ± 0.05	-1.20 ± 0.05	1.14 ± 0.05
$C_f(1.0)$ + latex	0.82%	$(1.8 \pm 0.2) \times 10^3$	-2.10 ± 0.08	0.24 ± 0.08	-2.10 ± 0.08	0.24 ± 0.08

carbon-fiber case than the steel-fiber case. The fact that the resistivity decrease is not large when the steel-fiber content is increased from 0.5% to 1.0% by weight of cement and the fact that the resistivity is still high at a steel-fiber content of 1.0% by weight of cement suggest that a steel-fiber content of 1.0% by weight of cement is below the percolation threshold.

Whether with or without silica fume (or latex), the change of the Seebeck voltage with temperature is more reversible and linear at a steel-fiber content of 1.0% by weight of cement than at a steel-fiber content of 0.5% by weight of cement. This is attributed to the larger role of the cement matrix at the lower steel-fiber content and the contribution of the cement matrix to the irreversibility and nonlinearity. Irreversibility and nonlinearity are particularly significant when the cement paste contains no fiber.

From the practical point of view, the steel-fiber silica-fume cement paste containing steel fibers in the amount of 1.0% by weight of cement is particularly attractive for use in temperature sensing, as the absolute thermoelectric power is the highest (68 $\mu V\,°C$) and the variation of the Seebeck voltage with the temperature difference between the hot and cold ends is reversible and linear. The absolute thermoelectric power is as high as those of commercial thermocouple materials.

Joints between concretes with different values of the thermoelectric power, as made by multiple pouring, provide concrete thermocouples [97].

6. Cement-matrix composites for thermal control

Concretes that are inherently able to provide heating through joule heating, provide temperature sensing (section 5), or provide temperature stability through a high specific heat (high thermal mass) are highly desirable for thermal control of structures and energy saving in buildings. Concretes of low electrical resistivity [69–78] are useful for joule heating, concrete thermistors and thermocouples are useful for temperature sensing, and concretes of high specific heat [66–68, 98] are useful for heat retention. These concretes involve the use of admixtures such as fibers and silica fume. For example, silica fume introduces interfaces which promote the specific heat [66]; short carbon fibers enhance the electrical conductivity [74] and render the concrete p-type [62]. (Plain concrete is n-type [62].) Comparative results shown in this section were obtained at similar moisture contents.

Figure 13 [74] gives the volume electrical resistivity of composites at 7 days of curing. The resistivity decreases greatly with increasing fiber volume fraction, whether a second filler (silica fume or sand) is present or not. When sand is absent, the addition of silica fume decreases the resistivity at all carbon-fiber volume fractions except the highest volume fraction of 4.24%; the decrease is most significant at the lowest fiber volume fraction of 0.53%. When sand is present, the addition of silica fume similarly decreases the resistivity, such that the decrease is most significant at fiber volume fractions below 1%. When silica fume is absent, the addition of sand decreases the resistivity only when the fiber volume fraction is below about 0.5%; at high fiber volume fractions, the addition of sand even increases the resistivity due to the porosity induced by the sand. Thus, the addition of a second filler (silica fume or sand) that is, essentially, non-conducting decreases the resistivity of the composite only at low volume fractions of the carbon fibers, and the maximum fiber volume fraction for the resistivity to decrease is larger when the particle size of the filler is smaller. The resistivity decrease is attributed to the improved fiber dispersion due to the presence of the second filler. Consistent with the improved fiber dispersion is the increased flexural toughness and strength due to the presence of the second filler.

Table 3 [67, 99] shows the specific heat of cement pastes. The specific heat is significantly increased by the addition of silica fume. It is further increased by the further addition of methylcellulose and defoamer. It is still further increased by the still further addition of carbon fibers. The effectiveness of the fibers in increasing the specific heat increases in the following order: as-received fibers, ozone-treated fibers, dichromate-treated fibers and silane treated fibers. This trend applies whether the silica fume is as-received or silane-treated. For any of the formulations, silane-treated silica fume gives higher specific heat than the as-received silica fume. The highest specific heat is exhibited by the cement paste with silane-treated silica fume and silane-treated fibers. The specific heat is 12% higher than that of plain cement

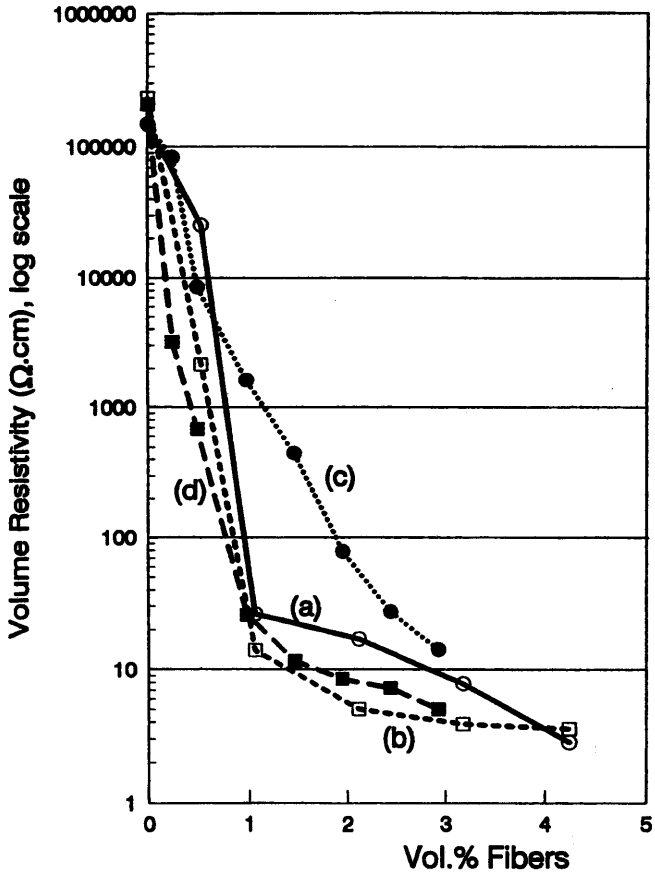

Figure 13. Variation of the volume electrical resistivity with carbon fiber volume fraction: (*a*) without sand, with methylcellulose, without silica fume; (*b*) without sand, with methylcellulose, with silica fume; (*c*) with sand, with methyscellulose, without silica fume; and (*d*) with sand, with methyscellulose, with silica fume.

Table 3. Specific heat (J g^{-1} K^{-1}, ±0.001) of cement pastes. The value for plain cement paste (with cement and water only) is 0.736 J g^{-1} K^{-1}. Note: A is cement + water + water reducing agent + silica fume; A^+ is A + methylcellulose + defoamer; A^+F is A^+ + as-received fibers; A^+O is A^+ + ozone-treated fibers; A^+K is A^+ + dichromate-treated fibers; and A^+S is A^+ + silane-treated fibers.

Formulation	As-received silica fume	Silane-treated silica fume
A	0.782	0.788
A^+	0.793	0.803
A^+F	0.804	0.807
A^+O	0.809	0.813
A^+K	0.812	0.816
A^+S	0.819	0.823

paste, 5% higher than that of the cement paste with as-received silica fume and as-received fibers, and 0.5% higher than that of the cement paste with as-received silica fume and silane-treated fibers. Hence, silane treatment of fibers is more valuable than that of silica fume for increasing the specific heat.

Table 4 [67, 99] shows the thermal diffusivity of cement pastes. The thermal diffusivity is significantly decreased by the addition of silica fume. The further addition of methylcellulose and defoamer or the still further addition of

Table 4. Thermal diffusivity (mm^2 s^{-1}, ±0.03) of cement pastes. The value for plain cement paste (with cement and water only) is 0.36 mm^2 s^{-1}. Note: A is cement + water + water reducing agent + silica fume; A^+ is A + methylcellulose + defoamer; A^+F is A^+ + as-received fibers; A^+O is A^+ + ozone-treated fibers; A^+K is A^+ + dichromate-treated fibers; and A^+S is A^+ + silane-treated fibers.

Formulation	As-received silica fume	Silane-treated silica fume
A	0.26	0.24
A^+	0.25	0.22
A^+F	0.27	0.26
A^+O	0.29	0.27
A^+K	0.29	0.27
A^+S	0.25	0.23

Table 5. Density (g cm^{-3}, ±0.02) of cement pastes. The value for plain cement paste (with cement and water only) is 2.01g cm^{-3}. A is cement + water + water reducing agent + silica fume; A^+ is A + methylcellulose + defoamer; A^+F is A^+ + as-received fibers; A^+O is A^+ + ozone-treated fibers; A^+K is A^+ + dichromate-treated fibers; and A^+S is A^+ + silane-treated fibers.

Formulation	As-received silica fume	Silane-treated silica fume
A	1.72	1.73
A^+	1.69	1.70
A^+F	1.62	1.64
A^+O	1.64	1.65
A^+K	1.65	1.66
A^+S	1.66	1.68

Table 6. Thermal conductivity (W m^{-1} K^{-1}, ±0.03) of cement pastes. The value for plain cement paste (with cement and water only) is 0.53 W m^{-1} K^{-1}. A is cement + water + water reducing agent + silica fume; A^+ is A + methylcellulose + defoamer; A^+F is A^+ + as-received fibers; A^+O is A^+ + ozone-treated fibers; A^+K is A^+ + dichromate-treated fibers; and A^+S is A^+ + silane-treated fibers.

Formulation	As-received silica fume	Silane-treated silica fume
A	0.35	0.33
A^+	0.34	0.30
A^+F	0.35	0.34
A^+O	0.38	0.36
A^+K	0.39	0.37
A^+S	0.34	0.32

fibers has relatively little effect on the thermal diffusivity. Surface treatment of the fibers by ozone or dichromate slightly increases the thermal diffusivity, whereas surface treatment of the fibers by silane slightly decreases the thermal diffusivity. These trends apply whether the silica fume is as-received or silane treated. For any of the formulations, silane-treated silica fume gives slightly lower (or essentially the same) thermal diffusivity than the as-received silica fume. Silane treatments of silica fume and of fibers are about equally effective for lowering the thermal diffusivity.

Table 5 [67, 99] shows the density of cement pastes. The density is significantly decreased by the addition of silica fume, which is used along with a water-reducing agent. It is further decreased slightly by the further addition of methylcellulose and defoamer. It is still further decreased

Table 7. Thermal behavior of cement pastes and mortars with and without silane treated silica fume.

	Cement paste		Mortar	
	Without silica fume	With silica fume	Without silica fume	With silica fume
Density ($g\ cm^{-3}$, ± 0.02)	2.01	1.73	2.04	2.20
Specific heat ($J\ g^{-1}\ K^{-1}$, ± 0.001)	0.736	0.788	0.642	0.705
Thermal diffusivity ($mm\ s^{-1}$, ± 0.03)	0.36	0.24	0.44	0.35
Thermal conductivity[a] ($W\ m^{-1}\ K^{-1}$, ± 0.03)	0.53	0.33	0.58	0.54

[a] Product of density, specific heat and thermal diffusivity.

Table 8. Loss tangent ($\tan \delta$).

	Frequency			
Mix	0.2 Hz	0.5 Hz	1.0 Hz	2.0 Hz
Plain	0.016 ± 0.01	$<10^{-4}$	$<10^{-4}$	$<10^{-4}$
Sand	$<10^{-4}$	$<10^{-4}$	$<10^{-4}$	$<10^{-4}$
Sand + silica fume	0.021 ± 0.01	0.14 ± 0.01	0.01 ± 0.01	$<10^{-4}$

Table 9. Storage modulus (GPa, ± 0.2).

	Frequency			
Mix	0.2 Hz	0.5 Hz	1.0 Hz	2.0 Hz
Plain	13.7	14.48	14.02	14.00
Sand	9.43	11.67	10.32	9.56
Sand + silica fume	13.11	14.34	13.17	13.11

by the still further addition of fibers. The effectiveness of the fibers in decreasing the density decreases in the following order: as-received fibers, ozone-treated fibers, dichromate-treated fibers and silane-treated fibers. This trend applies whether the silica fume is as-received or silane treated. For any of the formulations, silane-treated silica fume gives slightly higher (or essentially the same) specific heat as the as-received silica fume. Silane treatment of fibers is more valuable than that of silica fume for increasing the density.

Table 6 [67, 99] shows the thermal conductivity. It is significantly decreased by the addition of silica fume. The further addition of methylcellulose and defoamer or the still further addition of fibers has little effect on the density. Surface treatment of the fibers by ozone or dichromate slightly increases the thermal conductivity, whereas surface treatment of the fibers by silane has negligible effect. These trends apply whether the silica fume is as-received or silane treated. For any of the formulations, silane-treated silica fume gives slightly lower (or essentially the same) thermal conductivity as the as-received silica fume. Silane treatments of silica fume and of fibers contribute comparably to reducing the thermal conductivity.

Sand is a much more common component in concrete than silica fume. It is different from silica fume in its relatively large particle size and negligible reactivity with cement. Sand gives effects that are opposite from those of silica fume, i.e. sand addition decreases the specific heat and increases the thermal conductivity [98].

Table 7 [98] shows the thermal behavior of cement pastes and mortars. Comparison of the results on cement paste without silica fume and those on mortar without silica fume shows that sand addition decreases the specific heat by 13% and increases the thermal conductivity by 9%. Comparison of the results on cement paste with silica fume and those on mortar with silica fume shows that sand addition decreases the specific heat by 11% and increases the thermal conductivity by 64%. The fact that sand addition has more effect on the thermal conductivity when silica fume is present than when silica fume is absent is due to the low value of the thermal conductivity of cement paste with silica fume (table 7).

Comparison of the results on cement paste without silica fume and on cement paste with silica fume shows that silica-fume addition increases the specific heat by 7% and decreases the thermal conductivity by 38%. Comparison of the results on mortar without silica fume and on mortar with silica fume shows that silica-fume addition increases the specific heat by 10% and decreases the thermal conductivity by 6%. Hence, the effects of silica-fume addition on mortar and cement paste are in the same directions. The fact that the effect of silica fume on the thermal conductivity is much less for mortar than for cement paste is mainly due to the fact that silica-fume addition increases the density of mortar, but decreases the density of cement paste (table 7). The fact that the fractional increase in specific heat due to silica-fume addition is higher for mortar than cement paste is attributed to the low value of the specific heat of mortar without silica fume (table 7).

Comparison of the results on cement paste with silica fume and those on mortar without silica fume shows that sand addition gives a lower specific heat than silica-fume addition and a higher thermal conductivity than silica-fume addition. Since sand has a much larger particle size than silica fume, sand results in much less interface area than silica fume, although the interface may be more diffuse for silica fume than for sand. The low interface area in the sand case

Table 10. Loss tangent, storage modulus and loss modulus of mortars with and without steel reinforcement. Note the sample type designations are: A, No rebar; B, as-received steel rebar; C, ozone treated steel rebar; and D, sand blasted steel rebar.

Property	Sample type	Frequency		
		0.2 Hz	0.5 Hz	1.0 Hz
Loss tangent	A	$<10^{-4}$	$<10^{-4}$	$<10^{-4}$
	B	$(2.73 \pm 0.19) \times 10^{-2}$	$(1.56 \pm 0.08) \times 10^{-2}$	$(7.20 \pm 0.37) \times 10^{-3}$
	C	$(3.32 \pm 0.15) \times 10^{-2}$	$(1.98 \pm 0.17) \times 10^{-2}$	$(1.07 \pm 0.09) \times 10^{-2}$
	D	$(3.65 \pm 0.27) \times 10^{-2}$	$(2.50 \pm 0.22) \times 10^{-2}$	$(1.24 \pm 0.16) \times 10^{-2}$
Storage modulus (GPa)	A	20.2 ± 3.5	27.5 ± 4.3	25.8 ± 3.7
	B	44.2 ± 4.8	47.7 ± 5.3	44.4 ± 5.0
	C	36.9 ± 4.3	41.0 ± 3.9	38.4 ± 3.0
	D	46.0 ± 4.0	51.2 ± 6.4	49.3 ± 5.8
Loss modulus (GPa)	A	$<10^{-3}$	$<10^{-3}$	$<10^{-3}$
	B	1.21 ± 0.22	0.74 ± 0.12	0.32 ± 0.05
	C	1.23 ± 0.20	0.81 ± 0.15	0.41 ± 0.07
	D	1.68 ± 0.27	1.28 ± 0.27	0.61 ± 0.51

is believed to be responsible for the low specific heat and the higher thermal conductivity, as slippage at the interface contributes to the specific heat and the interface acts as a thermal barrier.

Silica-fume addition increases the specific heat of cement paste by 7%, whereas sand addition decreases it by 13%. Silica-fume addition decreases the thermal conductivity of cement paste by 38%, whereas sand addition increases it by 22%. Hence, silica-fume addition and sand addition have opposite effects. The cause is believed to be mainly associated with the low interface area for the sand case and the high interface area for the silica-fume case, as explained in the last paragraph. The high reactivity of silica fume compared to sand may contribute to causing the observed difference between silica-fume addition and sand addition, although this contribution is believed to be minor, as the reactivity should have tightened up the interface, thus decreasing the specific heat (in contrast to the observed effects). The decrease in the specific heat and the increase in the thermal conductivity upon sand addition are believed to be due to the higher level of homogeneity within a sand particle than within cement paste.

7. Cement-matrix composites for vibration reduction

Vibration reduction requires a high damping capacity and a high stiffness. Viscoelastic materials such as rubber have a high damping capacity but a low stiffness. Concretes having both high damping capacity (two or more orders higher than conventional concrete) (table 8) [100] and high stiffness (table 9) [100] can be obtained by using surface-treated silica fume as an admixture in the concrete. Steel-reinforced concretes having improved damping capacity and stiffness can be obtained by surface treating the steel (say by sand blasting) prior to incorporating the steel in the concrete (table 10) [101], or by using silica fume in the concrete [100]. Due to its small particle size, silica fume in concrete introduces interfaces which enhance damping. Sand blasting of a steel rebar increases the interface area between steel and concrete, thereby enhancing damping. Carbon-fiber addition has relatively small effects on the damping capacity and stiffness [102].

8. Cement-matrix composites for reflecting electromagnetic radiation

Cement-matrix composites containing 0.1 μm diameter discontinuous carbon filaments are effective for reflecting radio waves [80]. Due to the skin effect, conventional carbon fibers (7–15 μm diameter) are much less effective. The reflectivity renders the ability to shield electromagnetic interference (EMI) and to provide lateral guidance in the automatic highway technology [80].

9. Conclusion

Inherently smart structural composites for strain sensing, damage sensing, temperature sensing, thermal control, vibration reduction and radio wave reflection are attractive for smart structures. They are cement-matrix composites modified by using admixtures such as short carbon fibers, short steel fibers and silica fume. The electrical conductivity of the fibers enables the dc electrical resistivity of the composites to change in response to strain, damage or temperature, thereby allowing sensing. In addition, the conduction enables the Seebeck effect, which is particularly large in cement-matrix composites containing short steel fibers. By using the interfaces in composites to enhance damping, cement-matrix composites having both enhanced damping capacity and increased stiffness are obtained. By using composite interfaces, cement-matrix composites with increased specific heat for thermal control are also obtained.

Acknowledgment

This work was supported in part by National Science Foundation, USA.

References

[1] Newman J W 1987 *Int. SAMPE Symp. Exhib.* vol 32 (Covina, CA: SAMPE) pp 938–44

[2] Furukawa S, Tsuji Y and Otani S 1987 *Proc. 30th Japan Congress on Materials Research* (Kyoto: Society of Materials Science) pp 149–52

[3] Saito K, Kawamura N and Kogo Y 1989 Advanced materials: the big payoff *National SAMPE Technical Conf.* vol 21 (Covina, CA: SAMPE) pp 796–802
[4] Wen S and Chung D D L 1999 *Cen. Concr. Res.* **29** 445–9
[5] Sugama T, Kukacka L E, Carciello N and Stathopoulos D 1989 *Cem. Concr. Res.* **19** 355–65
[6] Fu X, Lu W and Chung D D L 1996 *Cem. Concr. Res.* **26** 1007–12
[7] Fu X, Lu W and Chung D D L 1998 *Carbon* **36** 1337–45
[8] Xu Y and Chung D D L 1999 *Cem. Concr. Res.* **29** 773–6
[9] Yamada T, Yamada K, Hayashi R and Herai T 1991 *Int. SAMPE Symp. Exhib.* vol 36 (Covina, CA: SAMPE) part 1, pp 362–71
[10] Sugama T, Kukacka L E, Carciello N and Galen B 1988 *Cem. Concr. Res.* **18** 290–300
[11] Larson B K, Drzal L T and Sorousian P 1990 *Composites* **21** 205–15
[12] Katz A, Li V C and Kazmer A 1995 *J. Mater. Civil Eng.* **7** 125–8
[13] Park S B and Lee B I 1993 *Cem. Concr. Composites* **15** 153–63
[14] Chen P, Fu X and Chung D D L 1997 *ACI Mater. J.* **94** 147–55
[15] Chen P and Chung D D L 1993 *Composites* **24** 33–52
[16] Brandt A M and Kucharska L 1996 Materials for the New Millennium *Proc. Mater. Eng. Conf.* vol 1 (New York: ASCE) pp 271–80
[17] Toutanji H A, El-Korchi T, Katz R N and Leatherman G L 1993 *Cem. Concr. Res.* **23** 618–26
[18] Banthia N and Sheng J 1996 *Cem. Concr. Composites* **18** 251–69
[19] Toutanji H A, El-Korchi T and Katz R N 1994 *Cem. Concr. Composites* **16** 15–21
[20] Akihama S, Suenaga T and Banno T 1984 *Int. J. Cem. Composites Lightweight Concrete* **6** 159–68
[21] Kamakura M, Shirakawa K, Nakagawa K, Ohta K and Kashihara S 1983 *Sumitomo Metals*
[22] Katz A and Bentur A 1994 *Cem. Concr. Res.* **24** 214–20
[23] Ohama Y and Amano M 1983 *Proc. 27th Japan Congress on Materials Research* (Kyoto: Society Materials Science) pp 187–91
[24] Ohama Y, Amano M and Endo M 1985 *Concrete Int.: Design Construction* **7** 58–62
[25] Zayat K and Bayasi Z 1996 *ACI Mater. J.* **93** 178–81
[26] Soroushian P, Aouadi F and Nagi M 1991 *ACI Mater. J.* **88** 11–18
[27] Mobasher B and Li C Y 1996 *ACI Mater. J.* **93** 284–92
[28] Banthia N, Moncef A, Chokri K and Sheng J 1994 *Can. J. Civil Eng.* **21** 999–1011
[29] Mobasher B and Li C Y 1994 Infrastructure: New Materials and Methods of Repair *Proc. Mater. Eng. Conf.* no 804 (New York: ASCE) pp 551–8
[30] Soroushian P, Nagi M and Hsu J 1992 *ACI Mater. J.* **89** 267–76
[31] Soroushian P 1990 *Construction Specifier* **43** 102–8
[32] Lal A K 1990 *Batiment Int./Building Research Practice* **18** 153–61
[33] Park S B, Lee B I and Lim Y S 1991 *Cem. Concr. Res.* **21** 589–600
[34] Park S B and Lee B I 1990 *High Temp.-High Pressures* **22** 663–70
[35] Soroushian P, Nagi M and Okwuegbu A 1992 *ACI Mater. J.* **89** 491–4
[36] Pigeon M, Azzabi M and Pleau R 1996 *Cem. Concr. Res.* **26** 1163–70
[37] Banthia N, Chokri K, Ohama Y and Mindess S 1994 *Adv. Cem. Based Mater.* **1** 131–41
[38] Banthia N, Yan C and Sakai K 1998 *Cem. Concr. Composites* **20** 393–404
[39] Urano T, Murakami K, Mitsui Y and Sakai H 1996 *Composites* A **27** 183–7
[40] Ali A and Ambalavanan R *Indian Concrete J.* **72** 669–75
[41] Chen P, Fu X and Chung D D L 1995 *Cem. Concr. Res.* **25** 491–6
[42] Zhu M and Chung D D L 1997 *Cem. Concr. Res.* **27** 1829–39
[43] Zhu M, Wetherhold R C and Chung D D L 1997 *Cem. Concr. Res.* **27** 437–51
[44] Chen P and Chung D D L 1993 *Smart Mater. Struct.* **2** 22–30
[45] Chen P and Chung D D L 1996 *Composites* B **27** 11–23
[46] Chen P and Chung D D L 1995 *J. Am. Ceram. Soc.* **78** 816–8
[47] Chung D D L 1995 *Smart Mater. Struct.* **4** 59–61
[48] Chen P and Chung D D L 1996 *ACI Mater. J.* **93** 341–50
[49] Fu X and Chung D D L 1996 *Cem. Concr. Res.* **26** 15–20
[50] Fu X, Ma E, Chung D D L and Anderson W A 1997 *Cem. Concr. Res.* **27** 845–52
[51] Fu X and Chung D D L 1997 *Cem. Concr. Res.* **27** 1313–8
[52] Fu X, Lu W and Chung D D L 1998 *Cem. Concr. Res.* **28** 183–7
[53] Wen S and Chung D D L *Cem. Concr. Res.* at press
[54] Shi Z and Chung D D L 1999 *Cem. Concr. Res.* **29** 435–9
[55] Mao Q, Zhao B, Sheng D and Li Z 1996 *J. Wuhan Univ. Tech., Mater. Sci. Ed.* **11** 41–5
[56] Mao Q, Zhao B, Shen D and Li Z 1996 *Fuhe Cailiao Xuebao/Acta Materiae Compositae Sinica* **13** 8–11
[57] Sun M, Mao Q and Li Z 1998 *J. Wuhan Univ. Tech., Mater. Sci. Ed.* **13** 58–61
[58] Zhao B, Li Z and Wu D 1995 *J. Wuhan Univ. Tech., Mater. Sci. Ed.* **10** 52–6
[59] Wen S and Chung D D L 1999 *Cem. Concr. Res.* **29** 961–5
[60] Sun M, Li Z, Mao Q and Shen D 1998 *Cem. Concr. Res.* **28** 549–54
[61] Sun M, Li Z, Mao Q and Shen D 1998 *Cem. Concr. Res.* **28** 1707–12
[62] Wen S and Chung D D L *Cem. Concr. Res.* at press
[63] Bontea D, Chung D D L and Lee G C *Cem. Concr. Res.* at press
[64] Wen S and Chung D D L *Cem. Concr. Res.* at press
[65] Lee J and Batson G 1996 Materials for the new millennium *Proc. 4th Mater. Eng. Conf.* vol 2 (New York: ASCE) pp 887–96
[66] Fu X and Chung D D L 1999 *ACI Mater. J.* **96** 455–61
[67] Xu Y and Chung D D L 1999 *Cem. Concr. Res.* **29** 1117–21
[68] Shinozaki Y 1990 Advanced materials: looking ahead to the 21st century *Proc. 22nd National SAMPE Tech. Conf.* vol 22 (Covina, CA: SAMPE) pp 986–97
[69] Fu X and Chung D D L 1995 *Cem. Concr. Res.* **25** 689–94
[70] Hou J and Chung D D L 1997 *Cem. Concr. Res.* **27** 649–56
[71] Clemena G G 1988 *Mater. Perform.* **27** 19–25
[72] Brousseau R J and Pye G B 1997 *ACI Mater. J.* **94** 306–10
[73] Chen P and Chung D D L 1993 *Smart Mater. Struct.* **2** 181–8
[74] Chen P and Chung D D L 1995 *J. Electron. Mater.* **24** 47–51
[75] Wang X, Wang Y and Jin Z 1998 *Fuhe Cailiao Xuebao/Acta Materiae Compositae Sinica* **15** 75–80
[76] Banthia N, Djeridane S and Pigeon M 1992 *Cem. Concr. Res.* **22** 804–14
[77] Xie P, Gu P and Beaudoin J J 1996 *J. Mater. Sci.* **31** 4093–7
[78] Shui Z, Li J, Huang F and Yang D 1995 *J. Wuhan Univ. Tech., Mater. Sci. Ed.* **10** 37–41
[79] Fu X and Chung D D L, *Cem. Concr. Res.* **28** 795–801
[80] Fu X and Chung D D L 1998 *Carbon* **36** 459–62
[81] Fu X and Chung D D L 1996 *Cem. Concr. Res.* **26** 1467–72
Fu X and Chung D D L 1997 *Cem. Concr. Res.* **27** 314
[82] Fujiwara T and Ujie H 1987 *Tohoku Kogyo Daigaku Kiyo, 1: Rikogakuhen* no 7 179–88
[83] Shimizu Y, Nishikata A, Maruyama N and Sugiyama A 1986 *Terebijon Gakkaishi/J. Inst. Television Eng. Japan* **40** 780–5 (1986).

[84] Chen P and Chung D D L 1996 *ACI Mater. J.* **93** 129–33
[85] Uomoto T and Katsuki F 1994–1995 *Doboku Gakkai Rombun-Hokokushu/Proc. Japan Soc. Civil Eng.* **490** 167–74
[86] Huang C M, Zhu D, Dong C X, Kriven W M, Loh R and Huang J 1996 *Ceramic Eng. Sci. Proc.* **17** 258–65
[87] Huang C M, Zhu D, Cong X, Kriven W M, Loh R R and Huang J 1997 *J. Am. Ceramic Soc.* **80** 2326–32
[88] Kim T-J and Park C-K 1998 *Cem. Concr. Res.* **28** 955–60
[89] Igarashi S and Kawamura M 1994 *Doboku Gakkai Rombun-Hokokushu/Proc. Japan Soc. Civil Eng.* **502** 83–92
[90] Bayasi M Z and Zeng J 1997 *ACI Structural J.* **94** 442–6
[91] Campione G, Mindess S and Zingone G 1999 *ACI Mater J.* **96** 27–34
[92] Yamada T, Yamada K and Kubomura K 1995 *J. Composite Mater.* **29** 179–94
[93] Delvasto S, Naaman A E and Throne J L 1986 *Int. J. Cem. Composites Lightweight Concr.* **8** 181–90
[94] Park C 1998 *Nippon Seramikkusu Kyokai Gakujutsu Ronbunshi - J. Ceram. Soc. Japan* **106** 268–71
[95] Shao Y, Marikunte S and Shah S P 1995 *Concr. Int.* **17** 48–52
[96] Wen S and Chung D D L *Cem. Concr. Res.* at press
[97] Wen S and Chung D D L *Cem. Concr. Res.* at press
[98] Xu Y and Chung D D L, *Cem. Concr. Res.* at press
[99] Xu Y and Chung D D L *ACI Mater. J.* at press
[100] Wang Y and Chung D D L 1998 *Cem. Concr. Res.* **28** 1353–6
[101] Wen S and Chung D D L *Cem. Concr. Res.* at press
[102] Xu Y and Chung D D L 1999 *Cem. Concr. Res.* **29** 1107–9